Experimental Study of the $O^{17}(p,\alpha)N^{14}$ Reaction and a Calculation of the Rate of this Reaction in the CNO Cycle in Stars*

RONALD E. BROWN†
California Institute of Technology, Pasadena, California
(Received August 7, 1961)

An experimental measurement of the absolute cross section for the $O^{17}(p,\alpha)N^{14}$ reaction has been carried out in the energy range from 490- to 1580-kev proton bombarding energy at a laboratory angle of 150°. Resonances were observed at proton energies of 518, 672, 747, 825, 927, 1096, 1101, 1247, 1274, and 1335 kev. Other level parameters were assigned where possible. The 747-kev resonance corresponds to a level in F^{18} at 6302-kev excitation which does not appear to have been previously reported. A calculation of the ratio O^{17}/O^{16} formed at equilibrium at various temperatures in the CNO cycle in stars is made, and it is concluded that the terrestrial material which has been processed in the CNO cycle underwent this processing at a temperature of about 17×10^6 °K.

I. INTRODUCTION

In recent years theoretical work on the properties of the mass-18 system[1–5] has stimulated a good deal of work on the levels of F^{18}—especially the low-lying levels.[6] In this work the results of an investigation of several of the higher levels of F^{18} by means of the $O^{17}(p,\alpha)N^{14}$ reaction is reported. Also reported is an application of our present knowledge of the F^{18} level structure to an estimate of the $O^{17}(p,\alpha)N^{14}$ reaction rate in stars.

In the present experiment an excitation curve at a laboratory angle of 150° was taken with protons ranging in energy from 490 to 1580 kev. This covers the region of excitation in F^{18} from 6.06 to 7.09 Mev. Below 1-Mev bombarding energy several very narrow, well isolated resonances were found, and above this energy several narrow anomalies superimposed on rather broad resonances were observed. Previous work on the $O^{17}(p,\alpha)N^{14}$ reaction had been carried out by Ahnlund[7] in the region of 1- to 3-Mev bombarding energy. In the present work, some structure near 1250 kev was seen that was not reported by Ahnlund.[7] The present work and the work of Ahnlund[7] are the only reported investigations of the $O^{17}(p,\alpha)N^{14}$ reaction to this date. This is presumably because the very low concentration (0.04%) of O^{17} in natural oxygen makes large enrichment factors necessary. Recently, enrichments of O^{17} of up to 4% have become available.[8]

Several other reactions have been used to investigate this region of excitation in F^{18}. The $F^{19}(He^3,\alpha)F^{18}$ reaction[9] has been used to measure the level positions in F^{18}. Several of the angular momentum and parity properties have been investigated by means of $N^{14}(\alpha,\alpha)N^{14}$ elastic scattering experiments.[10–14] Also investigated[10–12] have been $N^{14}(\alpha,p)O^{17}$ and[15] $N^{14}(\alpha,\gamma)F^{18}$. In Sec. V, some of these results will be compared with those obtained in the present experiment.

The importance of the $O^{17}(p,\alpha)N^{14}$ reaction in theories of element synthesis in stars comes from its occurrence in the well-known carbon-nitrogen-oxygen cycle (CNO cycle) in which it acts as a feedback into the main part of the cycle. The reactions occurring in the CNO cycle are[16]

$$\begin{aligned}&\rightarrow C^{12}(p,\gamma)N^{13}(\beta^+\nu)C^{13}\\ &\quad C^{13}(p,\gamma)N^{14}\\ &\rightarrow N^{14}(p,\gamma)O^{15}(\beta^+\nu)N^{15}\\ &\quad N^{15}(p,\alpha)C^{12}\\ &\quad \text{or } (1/2200)\\ &\quad N^{15}(p,\gamma)O^{16}\\ &\quad O^{16}(p,\gamma)F^{17}(\beta^+\nu)O^{17}\\ &\quad O^{17}(p,\alpha)N^{14}.\end{aligned}$$

Knowledge of the ratio of the amount of O^{16} to the amount of O^{17} formed in the CNO cycle then depends on a knowledge of the cross sections for $O^{16}(p,\gamma)$, which forms the O^{17}, and for $O^{17}(p,\alpha)$, which destroys it. This

* Supported in part by the joint program of the Office of Naval Research and the U. S. Atomic Energy Commission. This work is based on a thesis submitted to the California Institute of Technology in partial fulfillment of the requirements for the degree of Doctor of Philosophy.

† National Science Foundation Predoctoral Fellow. Present address: Department of Physics, University of Washington, Seattle, Washington.

[1] M. G. Redlich, Phys. Rev. **95**, 448 (1954).
[2] M. G. Redlich, Phys. Rev. **110**, 468 (1958).
[3] J. P. Elliott and B. H. Flowers, Proc. Roy. Soc. (London) **A229**, 536 (1955).
[4] J. P. Elliott, Proc. Roy. Soc. (London) **A245**, 128 (1958).
[5] J. P. Elliott, Proc. Roy. Soc. (London) **A245**, 562 (1958).
[6] F. Ajzenberg-Selove and T. Lauritsen, Nuclear Phys. **11**, 1 (1959).
[7] K. Ahnlund, Phys. Rev. **106**, 124 (1957).
[8] Weizmann Institute of Science, Rehovoth, Israel; Isomet Corporation, Palisades Park, New Jersey.
[9] S. Hinds and R. Middleton, Proc. Phys. Soc. (London) **73**, 721 (1959).
[10] N. P. Heydenburg and G. M. Temmer, Phys. Rev. **92**, 89 (1953).
[11] E. Kashy, P. D. Miller, and J. B. Risser, Phys. Rev. **112**, 547 (1958).
[12] D. F. Herring, R. Chiba, B. R. Gasten, and H. T. Richards, Phys. Rev. **112**, 1210 (1958).
[13] D. F. Herring, Phys. Rev. **112**, 1217 (1958).
[14] E. A. Silverstein, G. Hardie, L. Oppliger, and S. Salisburg, Bull. Am. Phys. Soc. **5**, 405 (1960).
[15] W. R. Phillips, Phys. Rev. **110**, 1408 (1958).
[16] W. A. Fowler, Mém. soc. roy. sci. Liège **16**, 207 (1960).

ratio is important in the light of a recent paper by Fowler, Greenstein, and Hoyle (FGH)[17] which discusses element formation in the early history of the solar system.

The present work thus consists of two main parts. In Secs. II through V, we discuss the experimental determination of the $O^{17}(p,\alpha)N^{14}$ cross section and the assignment of level parameters to the various states in F^{18}. Section VI deals with the astrophysical problem in the light of the suggestions of FGH.

II. EXPERIMENTAL AND ANALYTICAL PROCEDURES

The Kellogg Laboratory 2-Mv electrostatic generator was used to accelerate the protons for this experiment. The proton beam was rendered monoenergetic to about 0.2% by an 80° electrostatic analyzer and generator-voltage regulating system. A double-focusing magnetic spectrometer with an equilibrium orbit of 10.5 in.[18] was used to analyze the reaction products. A CsI(Tl) crystal and DuMont 6291 photomultiplier were used to detect those particles which pass through the spectrometer. The output pulses were displayed, after amplification, on a 10-channel pulse height analyzer.

The electrostatic analyzer was calibrated by an observation of the gamma rays produced by the $F^{19}(p,\alpha\gamma)O^{16}$ reaction occurring in a thick, evaporated CaF target as the proton bombarding energy was varied near a resonance in this reaction. The resonance energy was taken to be 872.7±0.4 kev.[19] The energy calibration and solid angle determination of the magnetic spectrometer were accomplished by an observation of the elastic scattering (assumed Rutherford) of 1-Mev protons from a thick, evaporated Cu target.

Two types of targets were used in the present measurements. One was a $\frac{1}{16}$-in. thick stainless steel disk which had been bombarded in a mass separator with O^{17} in the form of the ion $N^{14}O^{17}$. This resulted in a thin, nonuniform target of O^{17}. This target was brought to the Institute from Sweden by Ahnlund[7] for her investigation of the $O^{17}(p,\alpha)N^{14}$ reaction. Upon completion of her work here, she kindly left the target at the Institute. In what follows, this target will be referred to as the iron oxide target. The other type of target used was a thick, uniform, nickel oxide target. This type of target was prepared by oxidizing clean, polished, 15-mil thick nickel blanks in an induction heater. The oxygen gas used was obtained from the Weizmann Institute[8] and was of composition 3.97% O^{17}, 43.70% O^{18}, and 52.33% O^{16}. Their isotopic analysis has been assumed to be correct. At an early stage of the experiment, a sample of oxygen gas enriched to 2.77% O^{17} and 71.7% O^{18} was obtained from the Isomet Corporation.[8] The alpha-particle yield at several bombarding energies was found to be in the ratio 3.97/2.77 for targets made from the two gas samples, thus lending support to the above quoted O^{17} concentrations. From the observation of protons which were elastically scattered from the NiO targets, one can deduce that a surface layer of fully oxidized Ni was present and that this layer was about 26 kev thick to 1-Mev protons.

It will be seen in the following discussion that the iron oxide target and the nickel oxide targets complement one another in that they are suitable for data taking in different energy regions. The peak alpha-particle yield from the iron oxide target was found to be about four times that from the nickel oxide targets. The fact that the composition of the iron oxide target was not accurately known, however, precluded the measuring of absolute cross sections with this target. Thus only relative cross sections were measured with the iron oxide target—the results being normalized to the absolute measurements made with the nickel oxide targets. The fact that the iron oxide target was rather thin (about 6 kev thick to 1-Mev protons) compelled one to measure complete target profiles at each bombarding energy (the term target profile refers to counts vs spectrometer energy setting at fixed bombarding energy). The relations given by Snyder *et al.*[18] which relate thin-target yield to cross section were then used to obtain the relative cross sections. The proton reaction energy was determined by correcting the proton bombarding energy at the target surface (as determined from the electrostatic analyzer calibration) for energy loss in the body of the target, in the carbon contamination on the target surface at the beginning of a run, and in the carbon which was deposited on the target surface during a run. Where necessary, the target profiles also were corrected for carbon buildup during a run. Since the O^{17} distribution in the iron oxide target is a function of the spot that is being bombarded, it was not possible to shift target spots during a run. This made it difficult to obtain data near the very narrow resonances, because it was then difficult to correct for carbon buildup. The main advantage of the iron oxide target, therefore, lay in its relatively greater O^{17} concentration, and thus data were taken with this target in energy regions where the cross section does not vary rapidly with energy and where the cross section is quite low.

Even though the yield was lower for the nickel oxide targets, the majority of the data was taken with these targets. They are thick enough so that one may use the thick-target equations, as given by Snyder *et al.*,[18] which relate spectrometer yield to cross section. It is correct to use these equations as long as the spectrometer is set to detect only particles produced completely in the NiO region of the target. In order to avoid undesirable effects due to carbon buildup on the nickel oxide target surface, its position relative to the beam may be shifted as often as desired. This is especially important when one is

[17] W. A. Fowler, J. L. Greenstein, and F. Hoyle, Geophys. J. (to be published), (1961). This article is referred to by the abbreviation FGH.

[18] C. W. Snyder, S. Rubin, W. A. Fowler, and C. C. Lauritsen, Rev. Sci. Instr. **21**, 852 (1950).

[19] This value, which was used in the present work, should be compared with the value 872.5±0.4 kev adopted by J. B. Marion, Revs. Modern Phys. **33**, 139 (1961).

taking data at the narrow resonances. Thus the advantages of the nickel oxide targets are that they allow absolute cross-section measurements to be made and that the problem of carbon buildup on the target surface can be disposed of by shifting the target, whenever necessary, so that the proton beam bombards a new spot. The nickel oxide targets were used at all energies except at those where the cross section is quite low.

The proton reaction energy in the target can be determined from a formula given by Brown *et al.*[20] in which a knowledge of the magnetic spectrometer energy setting, the electrostatic analyzer energy setting, and the appropriate stopping cross sections allows one to calculate the reaction energy.

Because of the rather low counting rate in the present work, the entrance apertures and exit slits were removed from the magnetic spectrometer. This results in the largest possible solid angle, the highest counting rate, and the poorest energy resolution. The resolution in momentum $R=p/\Delta p$ was about 100 with all the exit slits removed. This results in an effective target thickness of approximately 3.5 kev to the incoming protons.

In addition to the alpha particles produced in the $O^{17}(p,\alpha)N^{14}$ reaction, there are also incident on the spectrometer elastically scattered protons and reaction products from target contaminants. Some of these undesired particles may pass through the spectrometer (either directly or by a series of scatterings) and be counted. The procedure for keeping track of these spurious counts plus the general background in the laboratory was somewhat different for the two types of targets. We first discuss the background determination for the nickel oxide targets.

For the nickel oxide targets the background was checked by bombarding a nickel oxide target which had been made with natural oxygen. Since the only difference between the natural and the enriched targets is in the relative concentrations of the oxygen isotopes, this method will correctly give the background except for effects resulting from O^{16} and O^{18}. No reaction products are produced by the O^{16} in the energy region under investigation here. The $O^{18}(p,\alpha)N^{15}$ reaction has a Q value of about 4 Mev as compared to that of 1.193 Mev for the $O^{17}(p,\alpha)N^{14}$ reaction.[21] The spectrometer will separate these two alpha-particle groups, and therefore the complete background was assumed to be given by the natural oxygen target. It was found that below 1.50-Mev bombarding energy the background ranged from about 5 to 20 counts per integration of 276 μcoul, depending on the bombarding energy and the general laboratory background at the time. This background is attributed both to laboratory background and to counts due to protons which scatter through the spectrometer and are counted. Above 1.50 Mev the background increases due to the increasing number of protons which pass through the spectrometer until at 1.583 Mev, the highest energy at which data were taken, the background was 50 counts per integration and the yield from the enriched target was 160 counts per integration. At the peaks of the narrow isolated resonances the counting rate from the enriched targets ranged from a low of 80 counts per integration at the 825-kev resonance to a high of 290 counts per integration at the 747-kev resonance. An example of the uncorrected data taken at the 672-kev resonance is shown in Fig. 1. The result of each integration is shown. In the data analysis the points at each energy were averaged together. The highest counting rate observed with the nickel oxide targets occurred at the peak of the broad 1274-kev resonance and amounted to 630 counts per integration of 276 μcoul.

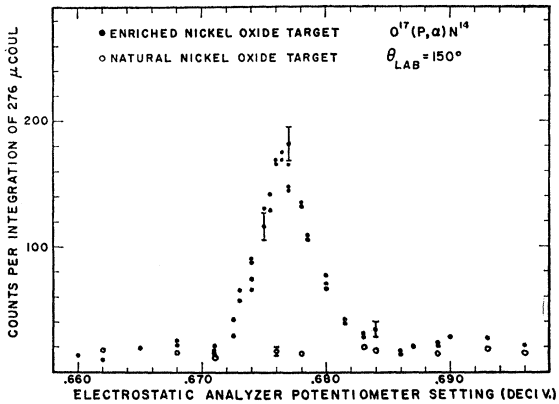

FIG. 1. Uncorrected data taken at the 672-kev resonance. The abscissa is proportional to the voltage on the plates of the electrostatic analyzer. The data in this figure were used to obtain the yield curve of Fig. 7.

We now discuss the background determination for the iron oxide target. For this target it was found that the target profiles do not go to zero counts when the spectrometer energy setting is such that no alpha particles from $O^{17}(p,\alpha)N^{14}$ should be observed. Instead it appeared as though there were a continuum of alpha particles underlying the $O^{17}(p,\alpha)N^{14}$ peak. By bombarding the back surface of the target, it was discovered that this continuum was being produced in the body of the stainless steel target backing. Figure 2, which is a target profile at a bombarding energy of 1.005 Mev, illustrates this effect. All background data for the iron oxide target were then taken by bombarding the back, unoxidized surface of the target. The target holder was arranged so that the front and back of the target could be bombarded alternately simply by rotating the target through 180°. In this way the same target spot was always brought back into the beam. No attempt was made to determine the actual reaction which was causing the continuum background.

The magnetic spectrometer was set to count the doubly charged alpha particles emerging from the target. However, these alpha particles undergo a suffi-

[20] A. B. Brown, C. W. Snyder, W. A. Fowler, and C. C. Lauritsen, Phys. Rev. 82, 159 (1951).

[21] F. Everling, L. A. Konig, J. E. Mattauch, and A. H. Wapstra, Nuclear Phys. 18, 529 (1960).

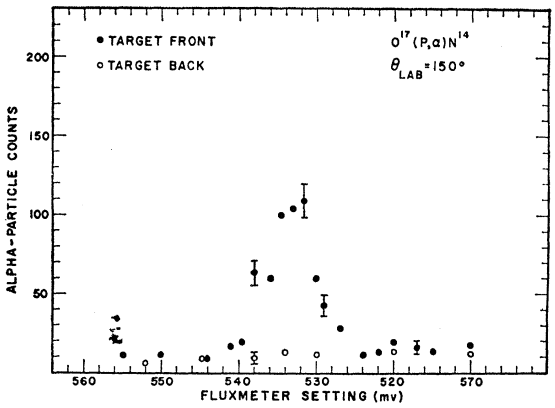

FIG. 2. Iron oxide target profile taken at a proton bombarding energy of 1,005 Mev. The abscissa is inversely proportional to the alpha-particle momentum. Each point represents an integrated beam current of 713 μcoul. Note: the setting 570 should read 510.

cient number of collisions in the target to reach charge equilibrium. Thus the number of doubly charged alpha particles which emerge from the target is less than the actual number produced by the reaction in the target. Therefore, the number of alpha particles which are counted must be corrected for this effect in order to obtain the true yield. The data given by Allison[22] for the charge equilibrium ratios of alpha particles in solids were used to obtain this correction.

The formulas[18,20] used to obtain the cross section and reaction energy from the data contain the stopping cross sections for the particles involved. The stopping cross sections needed here were obtained from the compilation of Whaling.[23] The stopping cross sections of nickel and of oxygen were added to obtain the stopping cross section of nickel oxide. Data on stopping cross sections for alpha particles are sparse, however, and Whaling's[23] compilation gives only proton values in nickel and oxygen. The alpha-particle stopping cross section $\epsilon_\alpha(E_\alpha)$ at energy E_α was computed from the proton stopping cross section $\epsilon_p(E_p)$ at energy E_p by use of the following equation:

$$\epsilon_\alpha(E_\alpha)=a\epsilon_p(E_p=E_\alpha/3.97). \quad (1)$$

Here a is a factor that ranged from 3.7 to 4.0 in the present experiment and is tabulated by Whaling[23] as a function of alpha-particle energy.

The error (standard deviation) in the scale of the absolute cross section in the present experiment is 10%. The bulk of this error is due to the uncertainty in the stopping cross section for the alpha particles. The error in the energy scale is $\frac{1}{3}$%.

III. EXPERIMENTAL RESULTS

Figure 3 shows the cross section per unit solid angle vs proton energy as determined in the present experiment. The experimental resolution was about 5 kev and was due to spectrometer resolution and energy straggling (see Sec. IV), and the data have not been corrected for this resolution. Therefore, the true cross section at the very narrow resonances rises to a higher value and has a narrower width than shown in Fig. 3. In order to more clearly display the lowest cross section values which were measured, a semilogarithmic presentation of the data between 600 and 1100 kev is given in Fig. 4. The vertical lines indicate the energy values at which narrow resonances occur. The data for these narrow resonances shown in Fig. 3 are not repeated in Fig. 4. Figure 5 shows the results near the broad resonances in some detail. The data for this figure have been converted to cross section and energy in the c.m. system. In Figs. 6, 7, and 8 is shown alpha-particle yield vs bombarding energy (i.e., proton energy at the target surface) for three of the narrow resonances observed in the present investigation. The yield curves for the other narrow resonances are similar to those shown here. The dashed curves appearing in Figs. 5 to 8 are theoretical curves and are discussed in Sec. IV.

IV. DETERMINATION OF LEVEL PARAMETERS

A. Broad Resonances

The cross section in the region E_p=1.0 to 1.5 Mev (Fig. 3) has been converted to c.m. cross section and c.m. energy E in the $O^{17}+p$ system. The results of this conversion are shown in Fig. 5. Here we describe how the resonance energies and widths of the high-yield broad resonance near E=1200 kev and of the low-yield broad resonance near E=1040 kev were determined. In this section the effects of the narrower anomalies at c.m. energies of 1040, 1177, and 1260 kev are neglected. The spin and parity of these broad levels are known to be 2^- and 1^- for the high-energy and low-energy levels, respectively, and both levels are known to decay by p-wave alpha particles.[6] It will be assumed here that the protons are also p-wave. Even though the levels

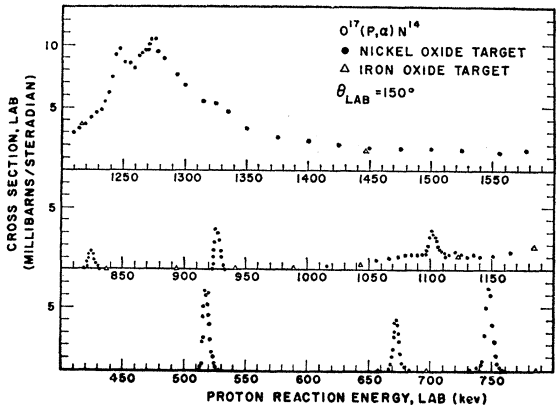

FIG. 3. Laboratory differential cross section vs proton energy. The experimental resolution was about 5 kev and is due to spectrometer resolution and energy straggling. The data in this figure have not been corrected for this resolution. The ordinate scale is accurate to 10%.

[22] S. K. Allison, Revs. Modern Phys. **30**, 1137 (1958).
[23] W. Whaling, *Handbuch der Physik*, edited by S. Flügge (Springer-Verlag, Berlin, 1958), Vol. 34, p. 193.

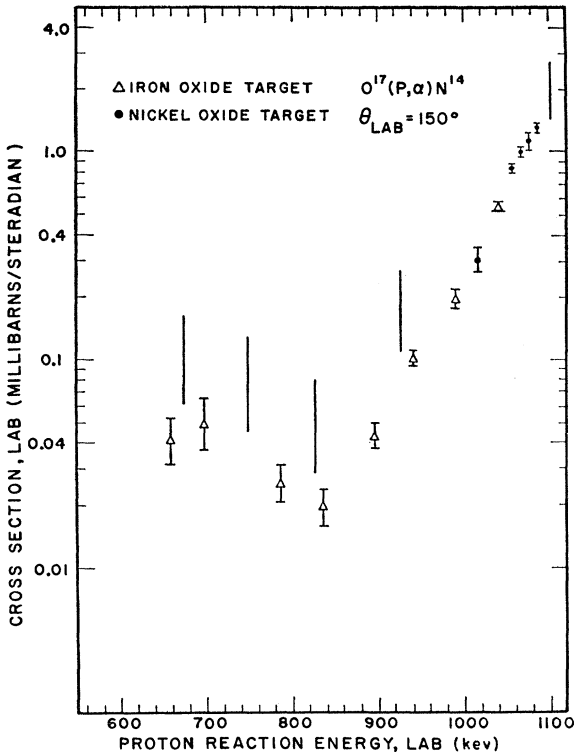

FIG. 4. Laboratory differential cross section vs proton energy in the energy region of lowest measured cross section. Note the logarithmic scale for the ordinate. The error bars indicate statistical errors only, and the absolute cross section scale is accurate to 10%. The vertical lines indicate the positions in energy of observed narrow resonances (see Fig. 3). As in Fig. 3, no corrections have been made for instrumental resolution.

have different spin, the cross section at a given angle (as opposed to the integrated cross section) will, in general, be expected to show interference effects between these two levels.[24] The correct general expression for the cross section will not be used here, however. Instead it will be assumed that a simple sum of two single-level contributions will suffice to determine the resonance energies and total widths to reasonable accuracy.[25] The energy variation of the level shift will be neglected, but the energy variation of the partial widths will be included. We then write

$$\sigma_{p\alpha}(152°)=\pi\lambda^2\left[\frac{\beta_1}{4\pi}g_1\frac{\Gamma_{1\alpha}\Gamma_{1p}}{(E-E_{r1})^2+\frac{1}{4}(\Gamma_{1\alpha}+\Gamma_{1p})^2}+\text{same term with } 1\rightarrow 2\right], \quad (2)$$

where 1 refers to the high-energy resonance and 2 refers to the low-energy resonance. Here g is the usual statistical weight factor; $g_1=5/12$ and $g_2=1/4$. Equation (2) refers to the cross section per unit solid angle in the c.m. system. The c.m. angle was very close to 152° over the range of energies employed in the present experiment. The anisotropy factor β_λ for a single level is defined by

$$\beta_\lambda=\left[4\pi\sigma(152°)\Big/\int\sigma(\theta)d\Omega\right]_{\text{single level}}. \quad (3)$$

The values used for the anisotropy factors were $\beta_1=1.00$ and $\beta_2=0.933$. The value for β_1 is based on the observed isotropy of the $N^{14}(\alpha,p)O^{17}$ reaction[11] for this level in F^{18}, and the value for β_2 is that calculated for a pure $J^\pi=1^-$ level associated with p-wave protons and p-wave alpha particles. The p-wave penetration factors for the proton channel and alpha particle channel were obtained from the graphs of Sharp *et al.*[26] The dimensionless reduced widths $\theta^2=Ma^2\gamma^2/\hbar^2$ and resonance energies E_r were varied until a "best fit" to the cross section was obtained.[27] This fit is shown as a dashed curve in Fig. 5. The channel radius a was taken to be given by $a=1.40(A_1^{\frac{1}{3}}+A_2^{\frac{1}{3}})$ fermi. For the proton channel this gives $a=5.000$ f and for the alpha-particle channel this gives $a=5.597$ f. Table I lists the total widths and resonance energies for the two resonances in question, along with parameters for the other resonances observed in the present work (see below). The partial widths are not uniquely determined from the data. Even if one assumes that Eq. (2) holds exactly

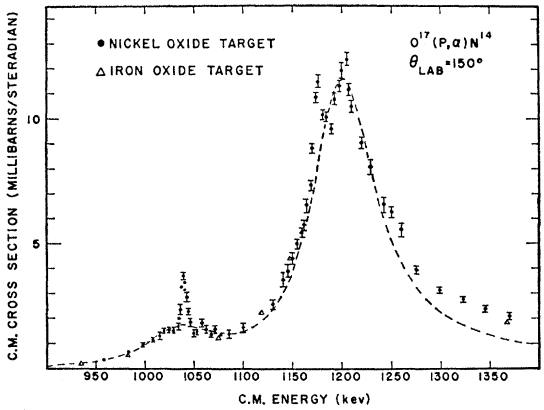

FIG. 5. Differential cross section in the c.m. system vs c.m. energy in the $O^{17}+p$ system. The figure shows the experimental results near the two broad resonances at c.m. energies of 1203 and 1035 kev (lab energies of 1274 and 1096 kev). The error bars indicate statistical errors only and the absolute cross section scale is accurate to 10%. The dashed curve was computed by a summing of two single level formulas in which the sharp resonances at 1040 and 1177 kev and the broader resonance at 1260 kev are neglected.

[24] A. M. Lane and R. G. Thomas, Revs. Modern Phys. **30**, 257 (1958).

[25] It is to be expected that such a procedure will give good accuracy for the high-yield resonance parameters and relatively poorer accuracy for the low-yield resonance parameters. No estimate of the effect of neglecting the interference was made however.

[26] W. T. Sharp, H. E. Gove, and E. B. Paul, Atomic Energy of Canada Ltd. Report AECL-268, 1955 (unpublished), 2nd ed.

[27] This "best fit" was determined by plotting the cross section as calculated from Eq. (2) along with the experimental values. The "best fit" was then determined by inspection and is therefore somewhat subjective.

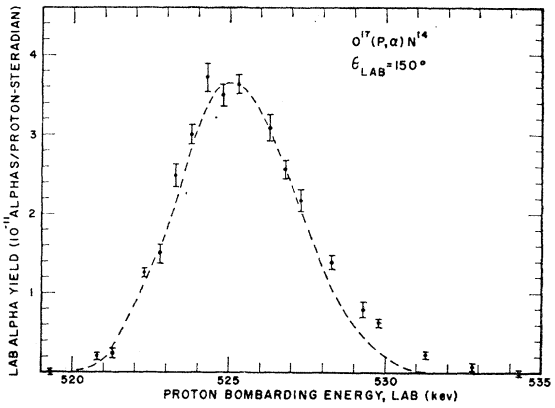

FIG. 6. Laboratory alpha-particle yield Y_L vs proton bombarding energy E_{1B} (at the target surface) near the 518-kev resonance. The error bars indicate statistical errors only. The dashed curve shows the expected yield from a narrow resonance when spectrometer resolution and energy straggling are taken into account in the manner discussed in the Appendix.

there is still an ambiguity as to whether or not it is the proton width or the alpha-particle width which is the largest. Table II gives the partial widths which are consistent with Eq. (2) and the data. The values in group I were used to calculate the dashed curve in Fig. 5. Group II could also have been used, however, as could a combination of I_a with II_b or I_b with II_a. This would result in only slight changes in the calculated cross section.

No analysis was performed on the resonance at $E=1260$ kev. The other two narrow levels appearing in Fig. 5 are discussed below.

B. Narrow Resonances

Three examples of the yield curves obtained at the narrow resonances are shown in Figs. 6 to 8. These curves and most of the others which are not shown here have a full width at half maximum of about 5 kev. One would like to know just how much of this width is due to the natural width of the resonance and how much is due to experimental effects. As was mentioned above, the spectrometer resolution can account for only about 3.5 kev of the observed width. Because the energy of the particle emerging from the target is a function of the angle, the nonzero angular acceptance of the spectrometer introduces an energy spread. This effect was calculated and found to be small in the present experiment. Finally, the effect of energy straggling of the incoming protons and outgoing alpha particles was investigated. In the Appendix is described a calculation of the yield in the laboratory Y_L as a function of the proton bombarding energy (at the target surface) E_{1B} for the case where a very high, very narrow (δ-function) resonance is responsible for the particle production. Gaussian functions are used for the straggling probabilities, and the spectrometer energy resolution is also taken into account. The results of the calculation, as illustrated by the dashed curves in Figs. 6 to 8, indicate that in most cases the bulk of the observed width can be attributed to energy straggling and spectrometer resolution with only a small contribution from the natural width of the resonance. For the 1247-kev (lab) resonance (yield curve not shown), however, a definite contribution from the natural width is observed, and for the 747-kev (lab) resonance (Fig. 8) there seems to be a smaller, but observable, contribution from the natural width.

One can notice a discrepancy between the calculated curves and the experimental data which occurs in the wings of the yield curves. In particular, the high-energy experimental points lie higher than the calculated curve. This is due to the fact that Gaussian distributions were used for the straggling functions and can be qualitatively explained in the following way. The actual straggling function is not Gaussian, but has a higher low-energy tail than a Gaussian.[28] Thus, at a high bombarding energy, more protons than calculated will slow down to the resonance energy by the time they reach the target lamina in which the main contribution to the spectrometer yield is produced. This would make the actual number of high-energy counts greater than calculated—as observed. A quantitative explanation would require the use of the correct straggling functions.[28]

It is quite easy to obtain the resonance energies from the data, but very difficult to extract the widths with any degree of accuracy. The area under the yield curves,

TABLE I. Summary of F^{18} level parameters as determined in the present experiment. The quantity $\beta g\Gamma_\alpha\Gamma_p/\Gamma$ is given in ev and all other quantities are expressed in kev.

E_r (lab)	E_r (c.m.)	E_{ex}	$\beta g\Gamma_\alpha\Gamma_p/\Gamma$	Γ (c.m.)
518±2	489±2	6086	50±5	<2.0
672±2	635±2	6232	43±4	<2.0
747±3	705±3	6302	100±10	3.1±1.4
825±3	779±3	6376	23±2	<4.5
927±3	875±3	6472	39±4	<1.2
1096±6	1035±6	6632		85±5
1101±4	1040±4	6637	36±4	<3.0
1247±5	1177±5	6774	150±16	10±3
1274±5	1203±5	6800		79±5
1335±10	1260±10	6857		

TABLE II. Partial widths for the two broad resonances occurring at c.m. energies of 1035 and 1203 kev (lab energies of 1096 and 1274 kev). The widths Γ_p and Γ_α are given in kev. Either group I or group II or a combination of I_a with II_b or I_b with II_a is consistent with the present data.

Group	E_r (c.m.)	θ_p^2	θ_α^2	Γ_p	Γ_α
I_a	1035	0.013	0.470	2.5	82.5
I_b	1203	0.194	0.060	64.5	14.5
II_a	1035	0.430	0.015	82.4	2.6
II_b	1203	0.044	0.267	14.5	64.5

[28] B. Rossi, *High-Energy Particles* (Prentice-Hall, Inc., New York, 1952).

however, can be measured quite accurately, and this area can be related to the resonance parameters. It is argued in the Appendix that the yield area is independent of the straggling. Thus the yield area is related in a simple manner to the true area under the resonance (see Eq. (A13)), which is, in turn, proportional to the quantity $\beta g\Gamma_a\Gamma_p/\Gamma$. The statistical factor is given by $g=(2J+1)/12$, and β is defined in Eq. (3). The quantity $\beta g\Gamma_a\Gamma_p/\Gamma$ in the c.m. system is given in Table I at the various narrow resonances observed in the present work. Also listed in this table are estimates of the total width for the resonances (in most cases, only an upper limit can be determined).

In the energy region below 1280-kev proton energy, the data were taken at small enough energy intervals so that an upper limit on the quantity $\beta g\Gamma_a\Gamma_p/\Gamma$ of 8 ev can be assigned to any unobserved narrow resonances. Above 1280 kev the data were taken in larger energy steps so it is possible that in the range from 1280 to 1580 kev some narrow resonances with $\beta g\Gamma_a\Gamma_p/\Gamma$ exceeding 8 ev are present.

V. DISCUSSION

In the subsequent discussion all quoted excitation energies E_{ex} in F^{18} are based on the mass differences[21] $O^{17}+H^1-F^{18}=5.597$ Mev and $N^{14}+He^4-F^{18}=4.404$ Mev.

All the levels observed in the present work (Table I) have been previously reported[6] except possibly the 747-kev level ($E_{ex}=6302$ kev). Hinds and Middleton[9] in a study of $F^{19}(He^3,\alpha)F^{18}$ report a level at 6264-kev excitation. This could possibly be the present 747-kev level since the alpha-particle group corresponding to their 6264-kev excitation was not completely resolved from the stronger group leading to the 6232-kev level in F^{18}.

The upper limits found here for the widths of the narrow levels are all consistent with previously reported limits. Width limits for the levels at $E_{ex}=6376$ and 6472 kev have not previously been reported. Also, the width of the level at $E_{ex}=6774$ kev had not previously been measured.

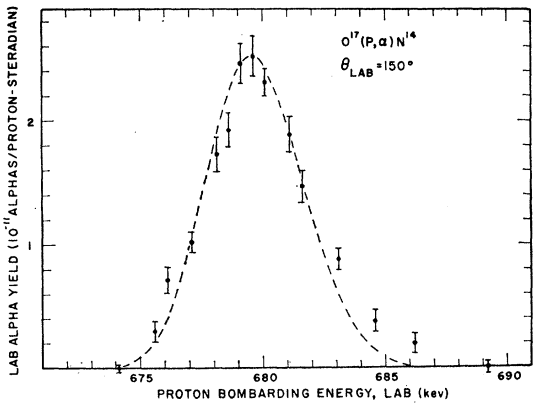

FIG. 7. Laboratory alpha-particle yield Y_L vs proton bombarding energy E_{1B} (at the target surface) near the 672-kev resonance. The error bars indicate statistical errors only. The dashed curve shows the expected yield from a narrow resonance when spectrometer resolution and energy straggling are taken into account in the manner discussed in the Appendix. The uncorrected data for this yield curve are shown in Fig. 1.

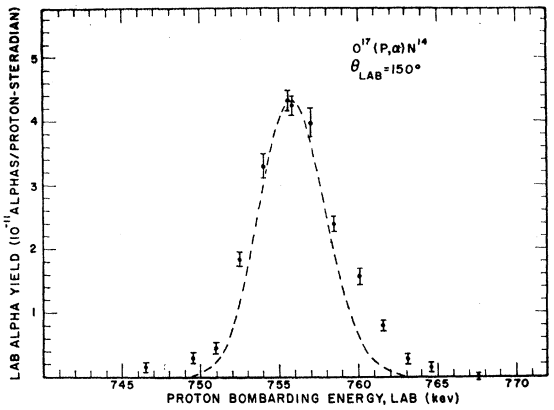

FIG. 8. Laboratory alpha-particle yield Y_L vs proton bombarding energy E_{1B} (at the target surface) near the 747-kev resonance. The error bars indicate statistical errors only. The dashed curve shows the expected yield from a narrow resonance when spectrometer resolution and energy straggling are taken into account in the manner discussed in the Appendix.

There have been several discrepancies in the literature concerning the widths of the broad levels at $E_{ex}=6632$ and 6800 kev. The results of the previous measurements of these widths along with those of the present work are given in Table III. Several of these discrepancies may easily be explained. It is clear from the papers of Ahnlund,[7] and Heydenburg and Temmer[10] that their quoted width for the 6800-kev level includes the contribution from the higher energy 6857-kev level. It is fairly certain that this is also the case for the value quoted by Herring.[13] In the work of Kashy *et al.*,[11] it is not clear whether or not their quoted value for the width of the 6800-kev level includes this extra contribution; however, they do not report a level at $E_{ex}=6857$ kev. In any case their value for this width is in agreement with the present work. By inspecting Fig. 5, one sees that if the contribution of the 6857-kev level were added to the width of the 6800-kev level as determined here, then one would obtain a value of about 100 kev in

TABLE III. Reported c.m. widths of the F^{18} levels at $E_{ex}=6632$ and 6800 kev. Previous determinations of these widths are compared with those of the present work. Widths are given in kev.

Investigators	6632-kev width (c.m.)	6800-kev width (c.m.)
Heydenburg and Temmer[a]	27±4	93±8
Ahnlund[b]		90
Herring[c]	93±5	101±5
Kashy, Miller, and Risser[d]	59±8	74±8
Present work	85±5	79±5

[a] See reference 10.
[b] See reference 7.
[c] See reference 13.
[d] See reference 11.

agreement with Heydenburg and Temmer[10] and with Herring.[13] The situation for the 6632-kev level is not so clear. The value of 27 kev may be discarded since it is clear that the narrow level at $E_{ex}=6637$ kev strongly influenced the data from which this width was derived. The present work agrees with Herring[13] and not with Kashy *et al.*[11] This is puzzling since the situation was simply reversed for the 6800-kev level. No completely satisfactory explanation for this fact has been found. One can safely say that the width values found in the present work are in agreement with those given by Herring[13] provided that his width for the 6800-kev level is taken to include the contribution from the 6857-kev level.

In the region of excitation of F^{18} under investigation in the present experiment, two levels have been previously reported in $N^{14}(\alpha,\alpha)N^{14}$ which were not seen in the present work. These are a level at $E_{ex}=6247$ kev[12–14] and one at $E_{ex}=6556$ kev.[12,13] The 6247-kev level is known to be formed by s-wave alpha particles yielding a 1^+ level in F^{18}. This would require that d-wave or g-wave protons form the state. The absence of this level in the present experiment can perhaps be explained on the basis of angular momentum considerations since one finds that Γ/θ^2 drops by a factor of 20 on going from p-wave to d-wave protons at the energy for this level. The 6556-kev level is thought to be formed through g-wave alpha particles giving either 3^+, 4^+, or 5^+ for the level. The absence of this level in the present experiment is evidence for discarding the 3^+ possibility since a 3^+ level can be formed by s-wave protons, whereas a 4^+ or 5^+ level require protons of d-wave or higher.

To summarize the experimental results, we note that Fig. 3 shows the complete excitation curve for the $O^{17}(p,\alpha)N^{14}$ reaction as measured in the present work. Figures 4 and 5 show selected regions of this curve and Figs. 6 to 8 show examples of the alpha-particle yield curves obtained at the narrow resonances. Table I summarizes the level parameters as determined in this investigation and Table II lists a consistent set of partial widths for the two broad resonances. Any unobserved narrow resonances below a proton energy of 1280 kev have $\beta g\Gamma_a\Gamma_p/\Gamma<8$ ev.

VI. ASTROPHYSICAL PROBLEM

A. General Discussion

In a recent paper, Fowler, Greenstein, and Hoyle (FGH)[17] propose that the relative abundance of several of the elements which were present in the original material from which the solar system condensed was modified by spallation processes and neutron interactions during the formation of the planets. Among their conclusions is that the O^{17} abundance was not modified appreciably by these processes and that the present terrestrial ratio O^{17}/O^{16} should be the same as for the primitive material. We use the symbols of the elements to stand for either their relative abundances or the number of nuclei per cm^3, depending on the context. Following the notation of FGH, we let β stand for the original production ratio of O^{16} relative to C^{12} in helium burning in red giant stars, and we let f represent the fraction of the C^{12} and O^{16} thus formed which has been processed to equilibrium in the CNO cycle. If we add the O^{17} ratio to an equation given by FGH, we find

$$C^{12}:N^{14}:O^{16}:O^{17}=[1-f+0.024f(1+\beta)]:0.95f(1+\beta):[(1-f)\beta+0.02f(1+\beta)]:\gamma f(1+\beta), \quad (4)$$

where the element symbols refer to the concentrations in the primitive material. This relation assumes that in the CNO cycle the equilibrium abundance ratios are given by

$$C^{12}:N^{14}:O^{16}:O^{17}=0.024:0.95:0.02:\gamma. \quad (5)$$

The numbers in Eq. (5) come from assuming equilibrium in the CNO cycle at a temperature of 35×10^6 °K. This rather high temperature results from the assumption that the last processing in the CNO cycle undergone by the O^{16} and C^{12} which were destined for the solar system took place in stars which were at a rather advanced stage of evolution. In these stars the hydrogen burning occurs in a thin high-temperature shell surrounding a helium core. We shall see below that the present calculation of the O^{17}/O^{16} ratio does not seem to agree with such a high temperature. FGH[17] next assume that the present solar abundance ratio[29] $C^{12}:N^{14}:O^{16}=5.5:1:9.6$ represents the original ratio of these nuclei in the primitive material. This assumption, along with Eq. (4) then leads to the values $\beta=1.75$ and $f=1/15$. From Eq. (4) one then finds

$$\frac{O^{17}}{O^{16}}=\frac{\gamma f(1+\beta)}{\beta(1-f)+0.02f(1+\beta)}=0.11\gamma. \quad (6)$$

The observed terrestrial ratio[30] is $O^{17}/O^{16}=3.74\times10^{-4}$ which leads to the value $\gamma=3.4\times10^{-3}$. The ratio at equilibrium in the CNO cycle is then given by Eq. (5) to be

$$[O^{17}/O^{16}]_{CNO}=\gamma/0.02=0.17. \quad (7)$$

Here we assume that the only possible way of forming O^{17} is through the CNO cycle.[31] The value of 0.17 is rather high and would result from a rather low rate for the O^{17}-destroying reaction, $O^{17}(p,\alpha)N^{14}$.

In the remainder of this section we obtain an expression for the low energy cross section for the $O^{17}(p,\alpha)N^{14}$ reaction and use this to calculate the ratio $[O^{17}/O^{16}]_{CNO}$ as a function of temperature. We then compare the results with the prediction of Eq. (7).

[29] L. Goldberg, E. A. Müller, and L. H. Aller, Suppl. Astrophys. J. **5**, No. 45 (1960).
[30] A. O. Nier, Phys. Rev. **77**, 789 (1950).
[31] E. M. Burbidge, G. R. Burbidge, W. A. Fowler, and F. Hoyle, Revs. Modern Phys. **29**, 547 (1957).

B. Cross-Section Factor and Reaction Rates at Stellar Energies

The observation of the very narrow levels at low energy in the present experiment leads one to suppose that these levels will have very little effect at energies of interest in stellar reactions (around 30-kev c.m. energy or 5627-kev excitation in F^{18}). One is then interested only in the effect of F^{18} levels which occur near this stellar energy region. A look at the F^{18} level scheme[6] indicates that only two of the known levels should be of importance in determining the stellar cross section for $O^{17}(p,\alpha)N^{14}$. These two levels occur at $E_{ex}=5594$ and 5662 kev (using the mass differences quoted at the beginning of Sec. V).

The 5594-kev level has been investigated by means of the $N^{14}(\alpha,\gamma)F^{18}$ reaction[15,32,33] and by means of the $N^{14}(\alpha,\alpha)N^{14}$ reaction.[14] All results point to a spin and parity assignment of 1^- for this level. Silverstein *et al.*[14] report that the alpha particles are p-wave and that the total width is about 200 ev.

The 5662-kev level has also been investigated by means of the $N^{14}(\alpha,\gamma)F^{18}$ reaction[15,32] and by means of the $N^{14}(\alpha,\alpha)N^{14}$ reaction.[14] Silverstein *et al.*[14] again quote a width of about 200 ev and assign p-wave alpha particles to the level. 1^- is again favored.

In order to calculate the $O^{17}(p,\alpha)N^{14}$ cross section at stellar energies, we shall consider only the contribution of these two levels. Since they have the same spin and parity, the total cross section σ will exhibit interference between the two levels. We let 1 refer to the 5662-kev level and 2 refer to the 5594-kev level. The total cross section may then be written[24]

$$\sigma=\pi\lambda\!\!\!^{-2}g\left|\frac{(\Gamma_{1p}\Gamma_{1\alpha})^{\frac{1}{2}}}{(E_{r1}-E)-i\Gamma_1/2}\pm\text{same term with } 1\rightarrow 2\right|^2, \quad (8)$$

where the energy dependence of the level shift has been neglected, and the approximation that the level widths Γ_1 and Γ_2 are much less than the level spacing $E_{r1}-E_{r2}$ has been made. This approximation is quite good in the present case. We have here defined $(\Gamma_\alpha\Gamma_p)^{\frac{1}{2}}$ to be positive and are allowing the $\pm$ in Eq. (8) to take care of the interference effects. For $J=1$ we have $g=\frac{1}{4}$.

For the $O^{17}+p$ channel the energy E will be sufficiently low so that the following approximation for the proton width will be valid.

$$\frac{\Gamma_l}{\theta_l^2}=\frac{\pi E_a\exp(-bE^{-\frac{1}{2}})}{K_{2l+1}^2(x)}(1-\alpha_l E), \quad (9)$$

with $E_a=\hbar^2/2Ma^2$, $b=2\pi\eta E^{\frac{1}{2}}=2\pi(M/2)^{\frac{1}{2}}Z_1Z_0e^2/\hbar$, and $x=(8\rho\eta)^{\frac{1}{2}}=2(Z_1Z_0e^2/aE_a)^{\frac{1}{2}}$. $K_n(x)$ is the modified Bessel function of the second kind of order n, and α_l is given by Burbidge *et al.*[31] and amounts to -2.095×10^{-4} kev^{-1} for p-wave protons[34] in the $O^{17}+p$ channel. Equation (9) is derived by neglecting the contribution of the regular Coulomb function F_l to the penetration factor $1/(F_l^2+G_l^2)$ and then expanding the irregular Coulomb function G_l in an asymptotic series in $1/\eta^2$ while holding $x^2=8\rho\eta$ constant.[35]

The energy $E+Q$ in the $N^{14}+\alpha$ channel is not low enough to make use of the approximation given by Eq. (9). The energy variation of the p-wave alpha-particle widths in the $N^{14}+\alpha$ channel was determined from the graphs of Sharp *et al.*[26]

For charged particle reactions, it is convenient to define a quantity $S(E)$, the cross section factor, by

$$S(E)=E\sigma(E)\exp(bE^{-\frac{1}{2}}). \quad (10)$$

Combination of Eqs. (8), (9), and (10) then gives

$$S(E)=S_1(E)+S_2(E)\pm S_I(E), \quad (11)$$

with

$$S_1(E)=s(1-\alpha_l E)\frac{\theta_{1p}^2\Gamma_{1\alpha}}{(E-E_{r1})^2+\Gamma_1^2/4}, \quad (12)$$

$S_2(E)$ is the same as $S_1(E)$ with 1 replaced by 2. The interference term $S_I(E)$ is given by

$$S_I(E)=s(1-\alpha_l E)\times\frac{2(\theta_{1p}^2\theta_{2p}^2\Gamma_{1\alpha}\Gamma_{2\alpha})^{\frac{1}{2}}[(E_{r1}-E)(E-E_{r2})-\Gamma_1\Gamma_2/4]}{[(E-E_{r1})^2+\Gamma_1^2/4][(E-E_{r2})^2+\Gamma_2^2/4]}. \quad (13)$$

In these equations s is given by

$$s=gEE_a(\pi\lambda\!\!\!^{-})^2K_{2l+1}^2(x)=g\pi^2\hbar^4/[2MaK_{2l+1}(x)]^2. \quad (14)$$

The positive sign in Eq. (11) gives constructive interference between the levels and the minus sign gives destructive interference between the levels. For the present calculation we find $x=3.24$, $K_3(x)=0.0858$, $b=244.1$ kev$^{\frac{1}{2}}$, and $s=6.543\times10^7$ kev^2-barn.

Finally, one must have an estimate of the dimensionless reduced widths θ_p^2 and θ_α^2 for the two levels in question. The total width of these levels is almost certainly due to the alpha-particle width and so, on the basis of the work of Silverstein *et al.*,[14] we have that Γ_α is about 200 ev for the levels involved. For convenience, we take $\theta_\alpha^2=0.14$ for both levels. This gives $\Gamma_1=268$ ev and $\Gamma_2=154$ ev. In order to obtain an estimate of θ_p^2, we shall assume that the two levels which contribute to the stellar cross section have reduced widths similar to the low-energy levels observed in the present experiment. On analysis one finds that a value $\theta_p^2\theta_\alpha^2=1\times10^{-3}$ is a reasonable estimate for these low-energy levels. We thus assume that this value applies to the levels in the stellar energy region. The cross section is proportional to this factor, and any future revisions of this quantity

[32] P. C. Price, Proc. Phys. Soc. (London) **A68**, 553 (1955).
[33] E. Almqvist, D. A. Bromley, and J. A. Kuehner, Bull. Am. Phys. Soc. **3**, 27 (1958).
[34] It will be assumed that only p-wave protons are involved in the formation of the two levels in question.
[35] M. H. Hull, Jr., and G. Breit, *Handbuch der Physik*, edited by S. Flügge (Springer-Verlag, Berlin, 1959), Vol. 41, Part 1, p. 408.

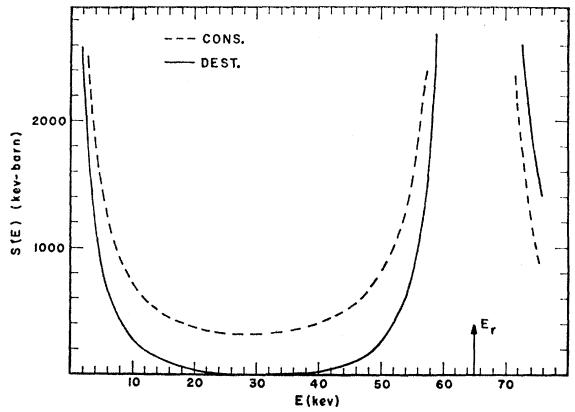

FIG. 9. Cross section factor $S(E)$ vs c.m. energy E in the $O^{17}+p$ system at the stellar energy region. Both the case of constructive interference and of destructive interference between the two contributing levels are shown. At the high-energy resonance, S rises to 6.88×10^6 kev-barn.

will result in an appropriate scale correction to the present calculations. The S factor may now be calculated. The results are shown in Fig. 9 for both the case of constructive and destructive interference between the levels.

One may now use the estimate of the cross section factor obtained above to compute the $O^{17}(p,\alpha)N^{14}$ reaction rate in stars. Since many authors (see Burbidge *et al.*[31] and references therein) have discussed the calculation of stellar reaction rates, no detailed derivations will be given here. One assumes that the reacting particles are at thermal equilibrium at absolute temperature T and possess a Maxwell-Boltzmann energy distribution. For charged particles, one makes use of Eq. (10) and obtains

$$\frac{P}{XY}=\left[\frac{8}{M(kT)^3}\right]^{\frac{1}{2}}\int_0^\infty dE\,S(E)\exp(-b/E^{\frac{1}{2}}-E/kT). \quad (15)$$

Here X and Y represent the number of nuclei per cm^3 of type X and Y, P is the reaction rate for X+Y in reactions per cm^3 sec, k is the Boltzmann constant, and M is the reduced mass of X and Y. The integral in Eq. (15) was evaluated graphically. In order to facilitate this, the effect of the resonance at $E=65$ kev was subtracted out and calculated separately. The rate correction P_c was then found graphically, where

$$P_c=P_{17}-P_r. \quad (16)$$

Here P_{17} is the total rate for the $O^{17}(p,\alpha)N^{14}$ reaction, and P_r is the contribution to the rate from the resonance at 65 kev. The formula for P_r is given by Burbidge *et al.*[31] This formula contains S_r, the S factor at resonance, which is equal to 6.88×10^6 kev-barn in the present calculation.

In order to check Eq. (7), the rate P_{16} for the $O^{16}(p,\gamma)F^{17}$ reaction is needed. The non-resonant approximation[31] was used to calculate this rate. An S_0 value of 5 kev-barn was used.[16]

The results of the rate calculations are given in Fig. 10 in the form of a plot of $\log(O^{17}P_{16}/O^{16}P_{17})$ vs temperature. Both the case of constructive and destructive interference for the $O^{17}(p,\alpha)N^{14}$ reaction are shown. The dashed curve shows the result when P_c is set equal to zero. Above 25 million degrees, the rate P_{17} is almost completely determined by the resonance at 65 kev in the $O^{17}(p,\alpha)N^{14}$ reaction. At equilibrium we have $P_{16}=P_{17}$; in which case the ordinate in Fig. 10 is just the logarithm of the ratio O^{17}/O^{16} in the CNO cycle. The top horizontal dashed line corresponds to the value for this ratio given by Eq. (7).

C. Discussion

On inspecting Fig. 10 we see that if the case of constructive interference applies, then a reduction of $\theta_p^2\theta_\alpha^2$ by a factor of 20 is necessary in order that $[O^{17}/O^{16}]_{CNO}$ reach the value given by Eq. (7). The case of destructive interference does reach the value of Eq. (7). If the present assumptions about the low energy cross section for the $O^{17}(p,\alpha)N^{14}$ reaction made above are correct, then it appears that the terrestrial material which has been processed in the CNO cycle underwent this processing at a considerably lower temperature than the 35 million degrees assumed in connection with Eq. (5). A reduction of $\theta_p^2\theta_\alpha^2$ by a factor of over 2000 for the higher level would be required to obtain $[O^{17}/O^{16}]_{CNO}=0.17$ at 35 million degrees. This is not impossible but seems unlikely in view of the experimental results of the present work. In order to be consistent, one should now compute $[O^{17}/O^{16}]_{CNO}$ at this lower temperature rather than use Eq. (7), which was based on an equilibrium temperature of 35 million degrees. Fowler[16] gives $C^{12}/N^{14}=0.01$ and $O^{16}/N^{14}=0.05$ at a temperature of 15 to 20 million degrees. These values do not change f, β, or γ appreciably, but $[O^{17}/O^{16}]_{CNO}$ is decreased to 0.072. The bottom horizontal dashed curve in Fig. 10 shows this ratio. It is seen that in the case of destructive interference this results in a shift of only about 1 million degrees in the processing temperature. Thus Fig. 10 shows that for destructive interference, a temperature of about 17 million degrees for the processing temperature in the CNO cycle appears to be consistent with the present calculations[36] and that about the same temperature would result if the constructive case applied and $\theta_p^2\theta_\alpha^2$ were reduced by a factor of 10.

A rough estimate of the remote-level contributions to $S(E)$ was made. If one assumes that $\theta_p^2\theta_\alpha^2=1\times10^{-3}$ also

[36] Calculations by Burbidge *et al.*, reference 31, would indicate that at temperatures given by the low-temperature intersections of the rate curve with the horizontal dashed lines the mean life of O^{16} is quite long and thus one would not expect equilibrium to be reached in the participation of O^{16} in the cycle. No investigation of the CNO cycle under nonequilibrium conditions has been carried out. Equilibrium conditions will almost certainly hold at high temperatures, however, so the present conclusion which excludes processing temperatures greater than 20 million degrees would seem to be a valid one.

holds for these levels, then one expects at most a contribution to the reaction rate of 40% of the minimum value found for the case of destructive interference. Thus it is expected that the above quoted processing temperature will be only slightly affected by distant levels.

In summarizing, we refer to Fig. 10 and point out that the terrestrial O^{17}/O^{16} ratio can be obtained if:

(a) Constructive interference applies with $\theta_p^2\theta_\alpha^2 \approx 10^{-4}$. This results in a maximum processing temperature for terrestrial material produced in the CNO cycle of about 20 million degrees.

(b) Destructive interference applies with $\theta_p^2\theta_\alpha^2 \approx 10^{-3}$. This gives a processing temperature of about 17 million degrees. A reduction of $\theta_p^2\theta_\alpha^2$ by a factor of 10 here would raise the temperature to about 20 million degrees.

(c) Either constructive or destructive interference applies and $\theta_p^2\theta_\alpha^2 \approx 10^{-6}$ with a processing temperature of about 35 million degrees.

It is felt that (c) and intermediate cases are somewhat unlikely and that the best estimate of the processing temperature is about 17 million degrees. At this temperature the equilibrium ratios are $C^{12}:C^{13}:N^{14}:N^{15}:O^{16}:O^{17} = 0.009:0.002:0.94:4\times10^{-5}:0.05:3\times10^{-3}$, while $f = 0.066$ and $\beta = 1.74$. It is suggested that nonequilibrium conditions in the CNO cycle should be investigated to determine this temperature more accurately, but it is expected that the temperature will not exceed 20 million degrees in any case. However, for nonequilibrium conditions, quite different abundance ratios than those given above may result.

ACKNOWLEDGMENTS

The author wishes to express his gratitude and thanks to the entire staff and personnel of the Kellogg Radiation Laboratory for their kind assistance during the course of this work. He is especially indebted to Professor William A. Fowler who suggested the problem and guided the work to its completion. Special thanks are also expressed to Barbara A. Zimmerman for her help with many of the computations.

APPENDIX

In this Appendix we derive an expression for the spectrometer yield from a thick target when both energy straggling and spectrometer resolution are taken into account. The case where the bombarding energy E_{1B} is varied over the region of a very narrow resonance is considered. We also briefly discuss the problem of the interpretation of the area under the yield curve.

Let $P_1(E_{1B},E_1;x)dE_1$ be the probability that the incoming particle, having a bombarding energy E_{1B}, will have an energy between E_1 and E_1+dE_1 after penetrating a distance x cm into the target. Let $P_2(E_2,E_{2S};x')dE_{2S}$ be the probability that the particle produced in the target at position x with energy

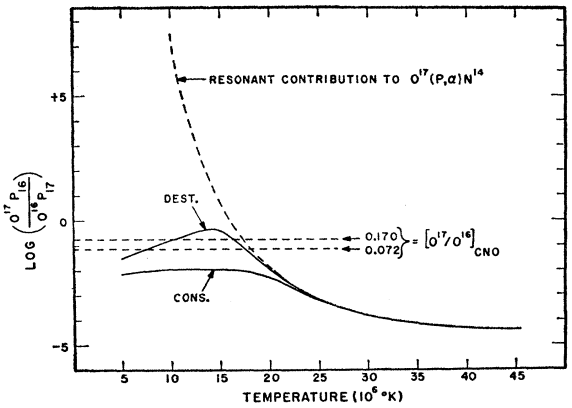

FIG. 10. Results of the calculations of the stellar reaction rates for $O^{17}(p,\alpha)N^{14}$ and $O^{16}(p,\gamma)F^{17}$ as described in Sec. VI. At equilibrium in the CNO cycle we have $P_{17}=P_{16}$ so that in this case the ordinate is just the logarithm of the isotopic ratio O^{17}/O^{16}. The horizontal dashed lines indicate such equilibrium ratios. Both the case of constructive and of destructive interference between the levels involved in the $O^{17}(p,\alpha)N^{14}$ reaction rate are shown. The dashed curve is what one obtains on assuming that the entire $O^{17}(p,\alpha)N^{14}$ reaction rate comes from the resonance at 65-kev.

$E_2=E_2(E_1)$ (determined from kinematics) will have energy between E_{2S} and $E_{2S}+dE_{2S}$ after passing a distance x' cm through the target. We shall be concerned with the case where the target normal bisects the angle between the incoming beam and the spectrometer position; thus $x=x'$. We let E_m stand for the spectrometer energy setting. The width in energy of the spectrometer window is then $2E_m/R$ where $R=p/\Delta p$ is the spectrometer momentum resolution. In the present experiment the target was raised to a potential $V_t=300$ v to prevent the escape of secondary electrons. If we define E_{20} by

$$E_{20}=E_m-Z_2eV_t, \tag{A1}$$

then we may calculate the laboratory yield $Y_L(E_{1B})$ in units of observed particles per bombarding particle per steradian by means of the relation

$$Y_L(E_{1B})=n\int_0^{E_{1B}}dE_1\int_0^X dx\int_{E_{20}-E_m/R}^{E_{20}+E_m/R}dE_{2S} \times P_1(E_{1B},E_1;x)P_2(E_2,E_{2S};x)\sigma(E_1), \tag{A2}$$

where n is the number of reacting nuclei per cm^3 in the target, X is the target thickness in cm and $\sigma(E_1)$ is the laboratory reaction cross section per unit solid angle evaluated at the energy E_1. The normalization condition on the probabilities $P(E,w;x)$ is

$$\int_0^E P(E,w;x)dw=1. \tag{A3}$$

We now make the following substitutions into Eq. (A2). We let

$$\sigma(E_1)=(\pi\sigma_r\Gamma/2)\delta(E_1-E_r), \tag{A4}$$

in order to obtain the effect of a very narrow resonance

at E_r. The normalization of the δ function is just the area under a narrow level of peak cross section σ_r and total width Γ. We next transform the x integral into a ξ integral, where

$$\xi = n_s \epsilon_{1r} x. \tag{A5}$$

Here n_s is the number of stopping molecules per cm^3 in the target, ϵ_{1r} is the stopping cross section per molecule (for the incoming particles) evaluated at $E=E_r$ (it is a good approximation to neglect the energy variation of the stopping cross section). Thus ξ is the average energy loss of the incoming particles after they have penetrated a depth x into the target. Finally, we approximate the straggling probabilities P_1 and P_2 by Gaussian functions with means of $E_{1B}-\xi$ and $E_{1B}-\xi\epsilon_{2r}/\epsilon_{1r}$, respectively, and with rms deviations Δ given by

$$\Delta^2 = z^2 \lambda_r \xi, \tag{A6}$$

with

$$\lambda_r = (4\pi e^4/\epsilon_{1r}) \sum Z_i, \tag{A7}$$

where Z_i is the charge of the stopping atoms and the sum is over the atoms in the stopping molecule. The condition for validity of the Gaussian approximation has been given by Rossi[28] and is that the rms deviation Δ must be large compared with the maximum transferable energy in a single collision, yet small compared with both the average energy at a distance x and the energy loss. In the present experiment it is found that the above condition is fairly well satisfied for the alpha particles but poorly satisfied for the protons. This is reflected in the discrepancy between the calculated yield and the experimental yield at the high-energy end (Figs. 6 to 8). After making the above-discussed substitutions into Eq. (A2) and performing the integration over the variables E_1 and E_{2S}, we find

$$Y_L(E_{1B}) = \frac{n\sigma_r\Gamma}{4n_s\epsilon_{1r}}\left(\frac{\pi}{2\lambda_r}\right)^{\frac{1}{2}} I(E_{1B}), \tag{A8}$$

with

$$I(E_{1B}) = \int_0^{\Xi} \frac{d\xi}{\xi}[\mathrm{erf}(L_+) - \mathrm{erf}(L_-)] \times \exp\left[\frac{-(E_r - E_{1B} + \xi)^2}{2\lambda_r \xi}\right], \tag{A9}$$

where

$$L_\pm = (E_{20} \pm E_m/R - E_{2r} + \xi\epsilon_{2r}/\epsilon_{1r})/(8\lambda_r\xi)^{\frac{1}{2}}. \tag{A10}$$

Here $E_{2r}=E_2(E_r)$, the error function is defined by

$$\mathrm{erf}(x) = \frac{2}{\sqrt{\pi}}\int_0^x \exp(-t^2)dt, \tag{A11}$$

and Ξ is the thickness of the target in energy to the incoming particles. The spectrometer setting E_m was changed as the bombarding energy E_{1B} was changed. The relation between these quantities was very closely linear so we may write

$$E_m = \alpha E_{1B} + \beta. \tag{A12}$$

The integral $I(E_{1B})$ was carried out on a Burroughs 220 computer for each of the seven narrow resonances (518 kev to 1241 kev) observed in the present work. The resonance energy E_r was chosen so that the peak of the calculated yield and that of the experimental yield falls at the same bombarding energy. The quantity $\sigma_r\Gamma$ in Eq. (A8) was chosen so that the peak value of the calculated yield coincides with the peak value of the experimental yield. Examples of three of these calculated yield curves are exhibited as dashed curves in Figs. 6 to 8.

We now briefly discuss the question of the relation of the yield area to the cross section parameters. It is not difficult to show that for a narrow resonance with no straggling, one obtains

$$\int Y_L(E_{1B})dE_{1B} = \left(\frac{\pi}{2}\sigma_r\Gamma\right)\frac{2nE_m(\max)}{n_s\epsilon_{1r}R(\alpha + \epsilon_{2r}/\epsilon_{1r})} \tag{A13}$$

with α given by Eq. (A12) and $E_m(\max)$ being the spectrometer setting at the maximum yield. The integration over E_{1B} was also carried out on the Burroughs 220 for the case where straggling is included, and Eq. (A13) was also found to hold for this case. The inclusion of a small natural width and the use of more accurate straggling functions in the calculation would not be expected to alter this conclusion to any significant extent. This then is the justification for the use of the no-straggling relation, Eq. (A13), in extracting the quantity $\beta g\Gamma_\alpha\Gamma_p/\Gamma$ from the actual yield area (see Sec. IV-B).

Mention should also be made of the fact that if one does not restrict the E_{2S} integration in Eq. (A2), but requires that one observe the entire outgoing particle spectrum, then the E_{2S} integration gives unity by virtue of Eq. (A3). The situation then reduces to that considered by Gove[37] in which he shows that the area is independent of energy spread in the beam or of straggling effects.

[37] H. E. Gove, *Nuclear Reactions*, edited by P. M. Endt and M. Demeur (Interscience Publishers, Inc., New York, 1959), p. 259.